GEOPHYSICAL RESEARCH LETTERS, VOL. 13, NO. 8, PAGES 721-724, AUGUST 1986

RUPTURE PROCESS OF THE MARCH 3, 1985 CHILEAN EARTHQUAKE

Douglas H. Christensen and Larry J. Ruff

Department of Geological Sciences, University of Michigan, Ann Arbor, MI 48109

Abstract. The March 3, 1985 central Chile earthquake (M_s= 7.8) ruptured a well studied seismic gap along the Chilean subduction zone. The epicenter of this event is located near the center of an approximately 300 km long region which ruptured in a great event in 1906 (M_w=8.2). The northern portion of the 1906 zone has since ruptured in 1971 (M_s=7.5) and 1973 (M_s=6.7). We have determined the rupture history of the 1985 central Chile earthquake from the deconvolved source functions of body waves (both P and PP). The source functions show one major pulse of moment release, the onset of which occurs about 16 seconds after an initial small pulse. The azimuthal directivity in the P waves indicates that the rupture front propagated from the epicenter southward and that the moment release of the major pulse is concentrated in a region between the epicenter and approximately 75 km south of the epicenter. We conclude that the region of high moment release is the dominant asperity and was loaded by slip in the relatively weaker northern region.

Introduction

The region between 32°S and 35°S (see Figure 1) along the central Chilean trench had been recognized as a mature seismic gap with a strong potential for large or great underthrusting earthquakes, based on historic seismicity (Kelleher, 1972; McCann et al., 1979; Nishenko, 1985). Previous great earthquakes occurred in this trench segment in 1647, 1730, 1822, and 1906, and give an average repeat time of 86±10 years (Nishenko, 1985). On July 9, 1971, the northern portion of the 1906 zone was ruptured by a large (M_s=7.5) underthrusting event. Although the 1971 event did not rerupture the complete 1906 zone, it may be considered the beginning of the next cycle of activity which may have culminated in the March 3, 1985 (M_s=7.8) earthquake (see Madariaga and Korrat, 1985). In addition to the historic evidence for a seismic gap, the authors (Christensen and Ruff, 1983) proposed that the occurrence of a large shallow compressional outer-rise event in this region on October 16, 1981 (M_s=7.2) indicated a build-up of compressional stress.

The epicenter of the March 3, 1985 earthquake (33.13°S, 71.87° W) is located at the southern end of the 1971 rupture zone in the same general region as the epicenter of the great 1906 earthquake. The focal mechanism (see Figure 1) which we use in this paper is the CMT (centroid moment tensor) solution from the Harvard group as listed in the PDE report (strike=11°, dip=26°, slip vector=110°) with a moment of 1.0×10^{28} dyne-cm. The depth extent of this event is somewhat difficult to determine. The Harvard and USGS moment tensor solutions give depths of 41 and 51 km, respectively, which are relatively deep for an underthrusting event. Sipkin (1985) finds a depth of 44 km from an unconstrained inversion of GDSN data. We have determined the depth extent by using the method described in Christensen and Ruff (1985). This method uses a "simplicity" criterion applied to the deconvolved source functions to find the best depth range. The results from eight stations shown in Figure 2 define a depth distribution with a lower bound of about 40 km. Although we will use a distributed source Green's function with a depth range of 10-40 km, a more restricted depth extent centered around 30 km cannot be ruled out by our method.

The one-day aftershocks were relocated by James Dewey and are plotted in Figure 1 (see Dewey et al., 1985). The aftershock region extends from about 32.5°S to about 34.25°S and seems to fill in an area which includes a large portion of the 1906 rupture zone, and overlaps the 1971 zone to the north. It should also be noted that the one-day aftershocks fall in a very narrow band at the down-dip edge of the coupled zone, and this pattern expands in the following months toward the trench, but does not expand along the trench axis. The aftershock pattern implies a rupture length of about 200 km and width of about 100 km. If we assume a fault area of 200x100 km^2 and a moment of 1.0×10^{28} dyne-cm, the average displacement over this area would be about 1.0 meter, which falls short of the tectonic accumulation of 7.2 meters since the 1906

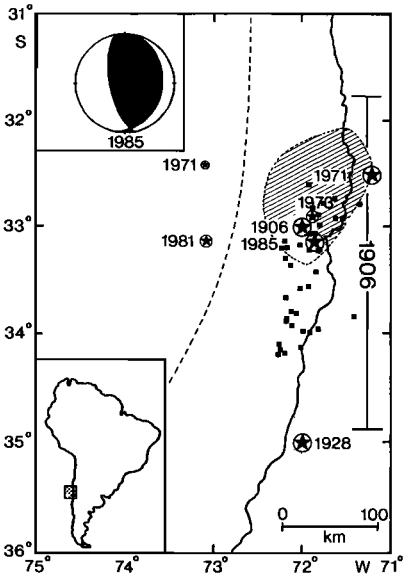

Fig. 1. Tectonic setting of the central Chile region, adapted from Nishenko (1985). The epicenters of large and great ($M_s \geq 7.5$) underthrusting events are shown as the large circled stars. Other smaller events are shown as the smaller circled stars. The aftershock zone from the 1971 underthrusting event is shown as the hachured area, and the relocated (after Dewey et al., 1985) one-day aftershocks for the March 3, 1985 event are shown as the small solid squares. The focal mechanism of the 1985 underthrusting event is shown on the top left, and the rupture extent of the great 1906 event is outlined by the vertical bar on the right.

Copyright 1986 by the American Geophysical Union.

Paper number 6L6156.
0094-8276/86/006L-6156$03.00

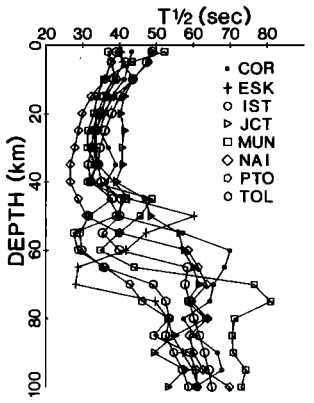

Fig. 2 Half-absolute moment time (T½) vs. depth curves for the Chile event of March 3, 1985. Each curve represents calculations from a single station. The best depth extent corresponds to low values of T½, with the deepest extent estimated by sharp increases in the T½ value.

event (convergence rate of 9.0 cm/yr). Discrepancies of this kind arise if, in reality, the moment release is concentrated in a smaller region. This region, known as an asperity, is then the strong region that accumulates the tectonic stress, while the surrounding weaker regions slip aseismically, or in series of smaller events.

In this paper we will examine the details of the rupture process of the March 3, 1985 Chile earthquake using deconvolved source functions from long-period P and PP waves.

P Wave Deconvolution and Rupture Process

We have deconvolved the source functions from 32 long-period WWSSN P and PP wave recordings, and the P and PP wave recordings from one special broadband station (ZUR), to determine the rupture process. The single-station deconvolution method is described in Ruff and Kanamori (1983); the source functions are deconvolved with a time interval of 2.0 seconds PP phases were utilized using the method outlined by Lynnes and Ruff (1985). The stations are well distributed azimuthally and thus allow for directivity analysis. Deconvolved source functions along with the observed and synthetic seismograms are shown in Figure 3. The source functions are remarkably simple for an event of this size, and quite consistent between stations. One major pulse of moment release is seen at all stations, preceded by a small amount of moment release with a duration of about 16 seconds A southward rupture direction is visually apparent in both the observed seismograms and in the deconvolved source functions (see Figure 3). A feature in the source functions can be located in space and time from the slight differences in the arrival time of the feature between stations. The method for locating a feature is the same as that used in Beck and Ruff (1984). For a specified rupture direction, the distance is given by the slope of the best-fit straight

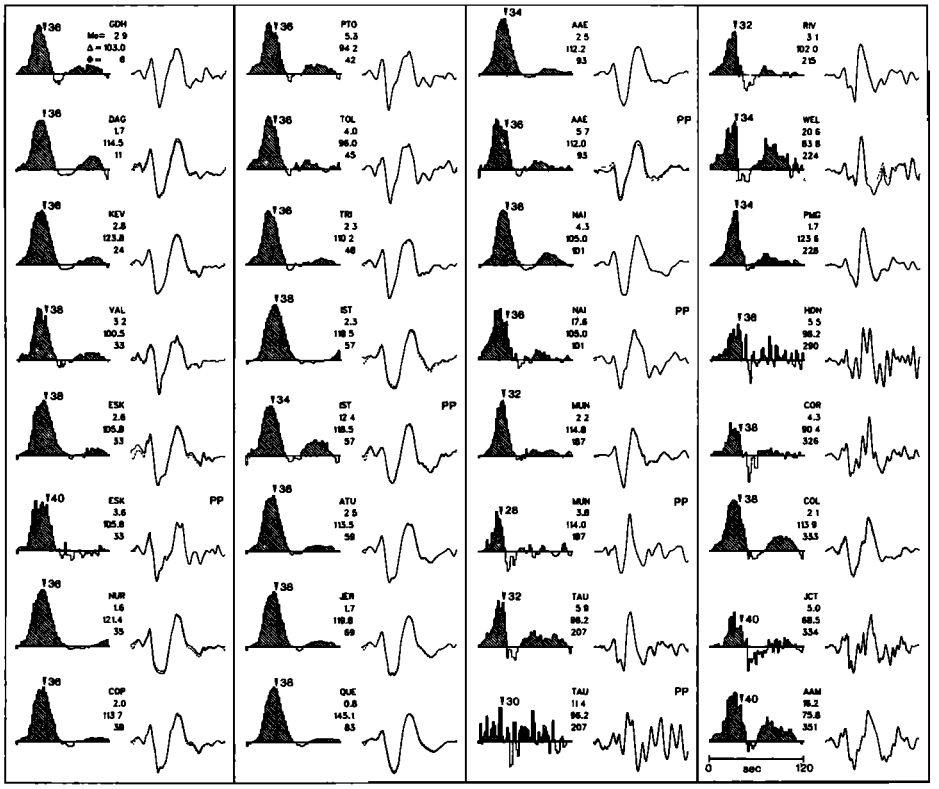

Fig. 3. Source functions deconvolved from P and PP phases for the March 3, 1985 earthquake. For each phase, the deconvolved source function is shown on the left and the observed and synthetic seismograms are on the right. The solid trace is the observed seismogram and the dashed trace is the synthetic seismogram calculated from the source function shown for each station. Hilbert transformed PP phases are labeled on the right. Station code, seismic moment (in 10^{27} dyne-cm), epicentral distance (in degrees) and azimuth (in degrees, clockwise from north) are listed for each source function. The delay time for the truncation of the main moment pulse which is used in the directivity study is marked on each source function.

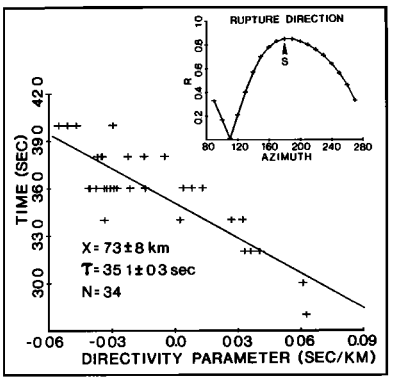

Fig. 4. Delay times for the truncation phase in the source functions shown in Figure 3, versus the directivity parameter (ray parameter multiplied by the cosine of the difference between the rupture direction and the station azimuth). A rupture direction of 180° produces the highest correlation coefficient. X is the distance from the epicenter to the truncation feature of the moment pulse, τ is the delay time relative to the rupture initiation, and N is the number of stations used in the calculation.

line of the delay times as a function of the directivity parameter (see Figure 4). The time axis intercept of the best-fit line is the true time delay of the feature relative to the origin time. The best rupture direction corresponds to the overall highest correlation between the delay times and the directivity parameter. The initiation of the main pulse, at about 16 seconds into the source function, displays no consistent directivity within the accuracy of our measurements (±2 seconds). This lack of detectable directivity suggests that the initiation of the main moment pulse is located within about 30 km of the epicenter. On the other hand, the truncation of the main moment pulse clearly shows directivity. The delay times of the truncation which are marked in Figure 3 are plotted in Figure 4 as a function of the directivity parameter for a rupture direction of 180° (due south, see Figure 4, inset). The directivity analysis shows that the main pulse truncation is located at 73±8 km (due south) from the epicenter with a delay time of 35 seconds. The rupture thus initiates near the epicenter and propagates to the south where it is truncated at about 75 km. The

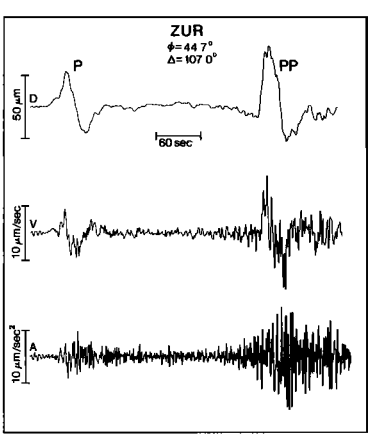

Fig. 5. Observed broadband data from station ZUR for P and PP phases of the March 3, 1985 earthquake. The three traces shown are the vertical component displacement (D), velocity (V), and acceleration (A).

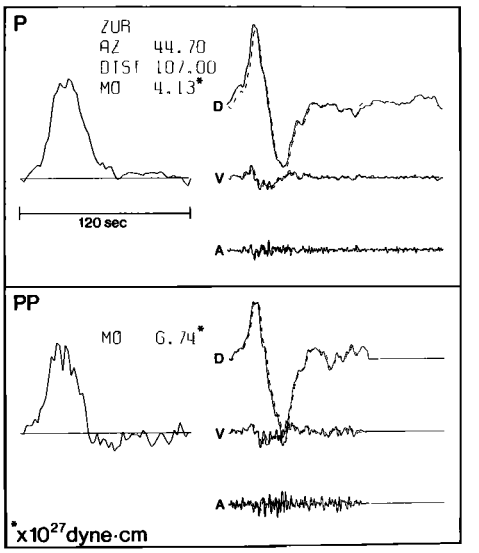

Fig. 6. Deconvolved source functions from the P wave (above) and Hilbert transformed PP wave (below) for the ZUR broadband displacement records. The observed and synthetic seismograms are shown by the solid and dashed lines, respectively.

main moment pulse in the source functions is released in this region, which represents the dominant asperity. The average rupture velocity between the origin and the main pulse truncation is 2 km/sec. While we observe no large pulses after the truncation, the one-day aftershock region extends 125 km southward of the epicenter and also 75 km to the north suggesting that the rupture continued into these regions. This implies that low-level moment release occurred over a broader area than the asperity. Indeed, the average moment in the main pulse of the deconvolved source

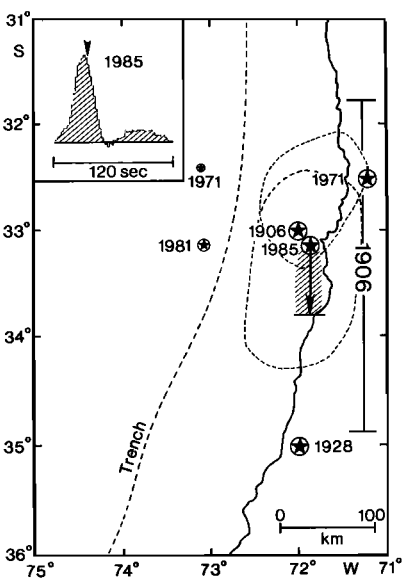

Fig. 7. Rupture process of the March 3, 1985 earthquake. The hachured area represents the asperity. The events shown are the same as described in Figure 1. The aftershock areas of the 1971 and 1985 underthrusting events are enclosed by the dashed lines. The average source function for the 1985 earthquake is shown in the top left corner.

functions from the undiffracted phases is $7x10^{27}$ dyne-cm, compared to the CMT moment of $1x10^{28}$ dyne-cm. If we allow the body wave moment from the main pulse to be released in the asperity region, assuming it to be 75 km long by 25 km wide, we then achieve the expected displacement of 7.2 meters calculated from the plate convergence. This type of behavior was also observed for the 1979 Colombia event (see Beck and Ruff, 1984).

Broadband Data

A broadband recording of the Chile earthquake from station ZUR in Switzerland was kindly provided by Dr. Erhardt Wielandt (see Wielandt and Streckeisen, 1982, for discussion of the instrument). The vertical component displacement, velocity, and acceleration traces for both the P and PP phases are shown in Figure 5. In Figure 6 we show the deconvolved source functions for both the P and the Hilbert transformed PP phases. Also shown in Figure 6 are the observed and predicted seismograms for all three traces. The source function is deconvolved from just the displacement record. The PP phase is undiffracted and clearly shows the added complexities of the higher frequencies. In particular the main pulse of moment release is "scalloped' with three crests. These higher frequency features probably correspond to the multiple source pulses reported by Houston and Kanamori (1985) and Choy (1985) in other broadband data. Hence, though this earthquake displays a comparatively smooth moment release, there are second-order complications in the major pulse of moment release.

Discussion and Conclusions

We now place our study of the rupture process in the context of the large events in the region. Our discussion starts with the August 16, 1906 (M_w=8.2) earthquake which ruptured a 300 km long segment of the subduction zone, thereby releasing the accumulated stress in this segment and partially loading the adjacent zones to the north and south. These adjacent regions subsequently ruptured in large events on December 1, 1928 (M_w=7.6) to the south, and on April 6, 1943 (M_w=8.2) to the north. The stress in the 1906 region increased due to the convergence between the Nazca and South American plates, until in 1971 the northern portion of the 1906 zone failed in the large underthrusting event of July 9, 1971 (M_s=7.5). The 1971 event had two important mechanical effects: first, it reduced the compressive stress in the immediate region as substantiated by the occurrence of a tensional outer-rise event just two months later (see Figure 1); and second, it transferred an additional load to the yet unruptured, relatively strong central portion of the 1906 zone. This additional loading is suggested by the occurrence of the large compressional outer-rise event on October 16, 1981 (M_s=7.2), and of course ultimately by the subsequent March 3, 1985 underthrusting event. The March 3, 1985 event nucleated at the southern end of the 1971 event and ruptured toward the south, releasing the majority of the moment between the epicenter and the truncation of the main moment pulse at about 75 km south of the epicenter (see Figure 7). We conclude that the dominant asperity in the 1906 segment lies in this region to the south of the 1971 "weak" zone. The 1906 segment ruptures with a fairly regular recurrence interval of 86±10 years, although the great events display a varying rupture length (see Kadinsky-Cade and Toksoz, 1985). This can be explained by the mechanical picture of a dominant asperity bounded by weak regions. The dominant asperity breaks with a regular interval, but the total extent of the rupture of this great event depends on the precursory events in the adjacent regions. It remains unclear whether the southern region of the 1906 zone (34.25°S-35°S) maintains a potential for a third event in this series or perhaps slipped prior to or during the 1985 event. Either way, the region south of the 1985 rupture zone, which includes the 1928 zone, becomes the next candidate for future large events.

Acknowledgments. We thank Dr. Erhardt Wielandt and many WWSSN station operators for providing the seismograms used in this study, and Dr. James Dewey for access to his aftershock relocations. This research was supported by grants from the National Science Foundation (EAR8407786) and the Shell Foundation.

References

Beck, S., and L. Ruff, The rupture process of the great 1979 Colombia earthquake: Evidence for the asperity model, *J. Geophy. Res., 89,* 9281-9291, 1984.

Choy, G.L., Source characteristics of the Chilean earthquake of March 3, 1985 and its aftershocks from broadband seismograms (abstract), *Eos Trans. AGU, 66,* 951, 1985.

Christensen, D.H., and L.J. Ruff, Outer-rise earthquakes and seismic coupling, *Geophys. Res. Lett., 10,* 697-700, 1983.

Christensen, D.H., and L.J. Ruff, Analysis of the trade-off between hypocentral depth and source time function, *Bull. Seismol. Soc. Am., 75,* 1637-1656, 1985.

Dewey, J.W., G.L. Choy, and S.P. Nishenko, Asperities and paired thrust zones in the focal region of the Chilean earthquake of March 3, 1985 (abstract), *Eos Trans. AGU, 66,* 950, 1985.

Houston, H., and H. Kanamori, The 1985 Valparaiso earthquake source spectrum (abstract), *Eos Trans. AGU, 66,* 950, 1985.

Kadinsky-Cade, K., and M.N. Toksoz, Rupture process and asperity distribution for the Central Chile M_s=7.8 earthquake of March 3, 1985 (abstract), *Eos Trans. AGU, 66,* 951, 1985.

Kelleher, J., Rupture zones of large South American earthquakes and some predictions, *J. Geophys. Res., 77,* 2087-2103, 1972.

Lynnes, C.S., and L.J. Ruff, Use of the PP phase to study the earthquake source, *Geophys. Res. Lett., 12,* 514-517, 1985.

Madariaga, R., and I. Korrat, Rupture of the Valparaiso (Chile) gap from 1971 to 1985 (abstract), *Eos Trans. AGU, 66,* 957, 1985.

McCann, W.R., S.P. Nishenko, L.R. Sykes, and J. Krause, Seismic gaps and plate tectonics: Seismic potential for major boundaries, *Pure Appl. Geophys., 117,* 1082-1147, 1979.

Nishenko, S.P., Seismic potential for large and great interplate earthquakes along the Chilean and southern Peruvian margins of South America: A quantitative reappraisal, *J. Geophys. Res., 90,* 3589-3616, 1985.

Ruff, L., and H. Kanamori, The rupture process and asperity distribution of three great earthquakes from long-period diffracted P-waves, *Phys. Earth Planet. Inter., 31,* 202-230, 1983.

Sipkin, S.A., Moment tensor analysis of the 1985 Chilean earthquake mainshock (abstract), *Eos Trans. AGU, 66,* 951, 1985.

Wielandt, E., and G. Streckeisen, The leaf-spring seismometer: Design and performance, *Bull. Seismol. Soc. Am., 72,* 2349-2367, 1982.

(Received April 18, 1986;
revised June 4, 1986;
accepted June 4, 1986.)